Age-Associated B Cells Express a Diverse Repertoire of V_H and Vκ Genes with Somatic Hypermutation

Lisa M. Russell Knode,* Martin S. Naradikian,† Arpita Myles,† Jean L. Scholz,† Yi Hao,†,1 Danya Liu,‡ Mandy L. Ford,‡ John W. Tobias,§ Michael P. Cancro,† and Patricia J. Gearhart*

The origin and nature of age-associated B cells (ABCs) in mice are poorly understood. In this article, we show that their emergence required MHC class II and CD40/CD40L interactions. Young donor B cells were adoptively transferred into congenic recipients and allowed to remain for 1 mo in the absence of external Ag. B cells expressing the T-bet transcription factor, a marker for ABCs, were generated after multiple cell divisions from C57BL/6 donors but not from MHC class II– or CD40-deficient donors. Furthermore, old CD154 (CD40L)-deficient mice did not accrue ABCs, confirming that they arise primarily through T-dependent interactions. To determine what Igs ABCs express, we sequenced V_H and Vκ rearranged genes from unimmunized 22-mo-old C57BL/6 mice and showed that they had a heterogeneous repertoire, which was comparable to that seen in old follicular and marginal zone B cell subsets. However, in contrast to the follicular and marginal zone cells, ABCs displayed significant somatic hypermutation. The mutation frequency was lower than found in germinal center cells after deliberate immunization, suggesting that ABCs have undergone mild stimulation from endogenous Ags over time. These observations show that quiescent ABCs are Ag-experienced cells that accumulate during T cell–dependent responses to diverse Ags during the life of an individual. ***The Journal of Immunology*****, 2017, 198: 1921–1927.**

Profound changes in the composition and dynamics of lymphoid populations occur with age, likely contributing to the decline in immune status, collectively termed immune senescence. For example, B cell production from bone marrow steadily decreases with age, yet the numbers of peripheral B cells remain relatively constant as a result of slowed turnover and altered representation of naive and Ag-experienced B cell subsets (1–8). A novel B cell subset that accumulates with age, termed age-associated B cells (ABCs), was identified recently (9–12). These cells have unique features that include preferential responsiveness to TLR7 and TLR9 ligands, surface markers consistent with prior Ag activation, and expression of the T-box transcription factor, Tbx21 (T-bet), which is required for their accumulation (13). Some ABCs also express Itgax (CD11c), an integrin that potentiates their ability to present Ag to T cells (14). ABCs are associated with the onset and severity of humoral autoimmunity in animal models and humans (10, 15, 16). Further, these cells play roles in age-associated immune dysfunctions, including elevated inflammatory cytokine levels and reduced B cell generation rates (11). Finally, a growing literature suggests that B cells with similar characteristics arise during some viral, bacterial, and parasitic infections (13, 17–21), implying a role for ABCs in normal immune function.

Despite these observations, the origin and nature of ABCs remain poorly understood. In this study, we investigated their formation, Ig repertoire, and level of somatic hypermutation. The results indicate a polyclonal, Ag-experienced B cell population that arises primarily through T-dependent immune responses to diverse endogenous Ags.

Materials and Methods

Mice

All mice used for experiments were females on a C57BL/6 background. Old mice were obtained from the Charles River aged mouse colony at 18 mo of age and used at 22 mo. *Cd154*$^{-/-}$ (B6.129S2-Cd40lg^{tm1Imx}/J) mice were purchased from the Jackson Laboratory and kept until 22 mo of age. Young (2–4 mo) CD45.1 and CD45.2 mice were obtained from the Jackson Laboratory. Young *I-Ab*$^{-/-}$ mice were from Terri Laufer (University of Pennsylvania), and *Cd40*$^{-/-}$ spleens from young mice were sent from M. Ford's colony. *Aid*$^{-/-}$ mice were bred in the National Institute on Aging colony. Animal protocols were reviewed and approved by the Animal Care and Use Committees at the National Institute on Aging and the University of Pennsylvania.

Adoptive transfers

CD23$^+$ splenic B cells from 2-mo-old CD45.2 mice were enriched by positive selection using the MACS bead system (Miltenyi Biotec). Cells

*Laboratory of Molecular Biology and Immunology, National Institute on Aging, National Institutes of Health, Baltimore, MD 21224; †Department of Pathology and Laboratory Medicine, Perelman School of Medicine, University of Pennsylvania, Philadelphia, PA 19104; ‡Emory Transplant Center and Department of Surgery, Emory University, Atlanta, GA 30322; and §Penn Molecular Profiling Facility, Perelman School of Medicine, University of Pennsylvania, Philadelphia, PA 19104

[1]Current address: Tongji Medical College, Wuhan, China.

ORCIDs: 0000-0003-1926-0382 (M.S.N.); 0000-0001-6103-6486 (D.L.); 0000-0002-5362-7013 (J.W.T.); 0000-0003-1975-4737 (P.J.G.).

Received for publication June 24, 2016. Accepted for publication December 20, 2016.

This work was supported by the Intramural Research Program of the National Institutes of Health, National Institute on Aging (to L.M.R.K. and P.J.G.) and by Grants PR130769 (Department of the Army) and R01 AG030227 (National Institute on Aging) (to M.P.C.). M.S.N. was supported in part by National Institute of Allergy and Infectious Diseases Grant T32 AI055428.

L.M.R.K., M.S.N., M.P.C., and P.J.G. designed experiments; L.M.R.K., M.S.N., A.M., Y.H., J.L.S., and J.W.T. performed research and analyzed data; D.L. and M.L.F. contributed reagents; and L.M.R.K., M.S.N., J.L.S, J.W.T., M.P.C., and P.J.G. wrote the manuscript.

Address correspondence and reprint requests to Dr. Michael P. Cancro or Dr. Patricia J. Gearhart, Department of Pathology and Laboratory Medicine, 284 John Morgan Building, 3620 Hamilton Walk, University of Pennsylvania, Philadelphia, PA 19104 (M.P.C.) or Laboratory of Molecular Biology and Immunology, National Institute on Aging, National Institutes of Health, 251 Bayview Boulevard, Baltimore, MD 21224 (P.J.G.). E-mail addresses: cancro@mail.med.upenn.edu (M.P.C.) or gearhartp@mail.nih.gov (P.J.G.)

The online version of this article contains supplemental material.

Abbreviations used in this article: ABC, age-associated B cell; AID, activation-induced deaminase; FO, follicular; HA, hemagglutinin; HA-PE, PE-labeled probe that recognizes HA of PR8; MZ, marginal zone; PR8, influenza strain A/Puerto Rico/8/1934.

were labeled with CFSE (eBioscience), according to the manufacturer's instructions, and 8 million cells were transferred into each CD45.1 congenic host by retro-orbital injection.

Flow cytometry and FACS sorting

Single-cell suspensions were prepared from spleens and stained with fluorochrome-conjugated Abs. For flow cytometry of the adoptive-transfer and influenza experiments, we used Live/Dead Zombie Aqua, anti-CD45.1-AF700 (A20), anti-CD45.2-BV421 (104), anti-CD19-BV785 (6D5), anti-CD23 biotin (B3B4), and anti-CD11c (N418) (BioLegend). Anti-CD43–PE (S7) was from BD Biosciences. Cells were analyzed on an LSRII, and data were analyzed using FlowJo software (TreeStar). Intracellular stains for T-bet were performed with anti–T-bet–allophycocyanin (4B10; BioLegend) and a Foxp3 transcription factor kit (eBioscience), according to the manufacturer's instructions. For FACS sorting to isolate subsets, we used anti-CD43–allophycocyanin (S7; BD Biosciences). Anti-CD23–PE Cy7 (B3B4), anti-CD21/CD35–eFluor 450 (4E3), anti-CD45R–FITC (B220, RA3-6B2), and anti-CD93 (AA4.1)-allophycocyanin were from eBioscience. Stained splenocytes were analyzed with a BD FACSCanto II or sorted using a BD FACSAria III, BD FACSAria Fusion, iCyt Reflection (Sony Biotechnology), or Beckman Coulter MoFlo. Follicular (FO) B cells were isolated as CD93 (AA4.1)$^-$ CD43$^-$ B220$^+$ CD21/35$^+$ CD23$^+$. Marginal zone (MZ) B cells were isolated as CD93 (AA4.1)$^-$ CD43$^-$ B220$^+$ CD21/35$^+$ CD23^{lo}. ABCs were isolated as CD93 (AA4.1)$^-$ CD43$^-$ B220$^+$ CD21/35$^-$ CD23$^-$. Analyses were done using FlowJo software.

V gene identification and mutation analyses

Sorted cells were lysed in TRIzol reagent, and RNA was prepared. cDNA was synthesized using SuperScript III Reverse Transcriptase (Invitrogen). Ig H chain VDJ genes and Ig κ light (Igκ)-chain VJ genes were amplified using Taq polymerase (TaKaRa; Clontech) with 5′ degenerate primers specific to framework 1 of V genes and 3′ primers located in IgM or Igκ constant regions, as previously described (22). PCR products were cloned into StrataClone TA cloning vector (Agilent Technologies) and sequenced. Only sequences with unique VDJ or VJ joins were counted. The sequences were blasted against the mouse Ig loci using IgBLAST from the National Center for Biotechnology Information to identify V, D, and J gene segment usage and mutations. For mutational analysis of the J_H4 intron, DNA was prepared, and a 492-bp intronic region downstream of J_H4 from rearranged V_HJ558 genes was amplified using nested PCR. The first round used forward primer J558 5′-AGCCTGACATCTGAGGAC-3′ and reverse primer V1.8NR4R 5′-TCCATACACATACTTCTGTGTTCCT-3′, and the second round used the same J558 forward primer listed above and reverse primer JH2827Bam 5′-CGCGGATCCGATGCCTTTCTCCCTTGACTC-3′. DNA was amplified using Herculase II Fusion DNA Polymerase (Agilent Technologies). The amplified PCR products were cloned into a StrataClone Blunt PCR Cloning vector (Agilent Technologies) and sequenced.

Influenza virus infection and analysis

Four-month-old C57BL/6 mice were left uninfected or infected intranasally with 30 tissue culture infectious $dose_{50}$ of influenza strain A/Puerto Rico/8/1934 (PR8), which was provided by Dr. S. Hensley (University of Pennsylvania). Both uninfected and infected mice were sacrificed 100 d later. To detect hemagglutinin (HA)-reactive B cells, we used a PE-labeled probe that recognizes HA of PR8 (HA-PE) (23). The probe was used at a concentration of 1:500, and data acquisition and analysis were performed as described (23).

Results

ABC generation requires B cell expression of MHC class II and CD40

We showed previously that ABCs could arise from FO B cells after in vivo expansion in adoptive hosts (9). This extensive division may reflect homeostatic expansion or could implicate Ag-driven activation involving T cell help and costimulation. To distinguish between these possibilities, we modified our adoptive-transfer model with CFSE-labeled donor B cells to use MHC class II– or CD40-deficient donor B cells. The rationale was that homeostatic expansion should be independent of Ag presentation and costimulation, whereas Ag-driven events should not. As shown in Fig. 1A, after 1 mo in the absence of immunization, a small proportion (~0.2%) of C57BL/6 donor B cells underwent five to eight rounds of division, likely in response to stimulation by endogenous Ags. These extensively divided CFSE^{lo} cells were CD23$^-$ and T-bet$^+$, which are markers for ABCs. Although the events occurred in only a month, they represent a snapshot of the slow accumulation of ABCs with time. In contrast, B cells from MHC class II–deficient (*I-Ab*$^{-/-}$) and CD40-deficient (*Cd40*$^{-/-}$) mice underwent fewer divisions with far less T-bet expression than

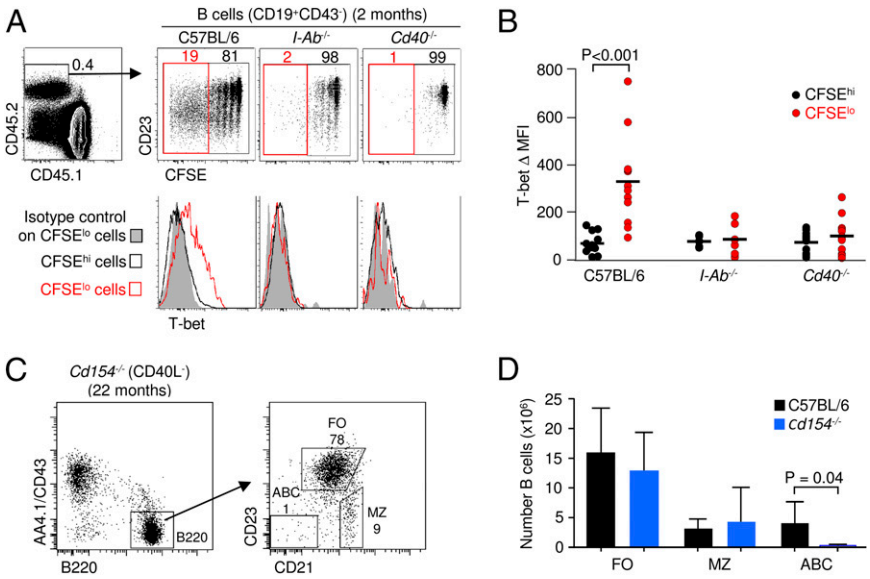

FIGURE 1. Interactions with MHC class II and CD40 drive the accumulation of ABCs. (**A**) CD23$^+$ FO B cells from 2-mo-old donor mice (CD45.2) were labeled with CFSE and adoptively transferred into young congenic CD45.1 hosts. Recipient mice were analyzed 1 mo later. Shown are a representative plot of the gating strategy and representative dot plots of CFSE dilution in C57BL/6, *I-Ab*$^{-/-}$, and *Cd40*$^{-/-}$ cells. Numbers depict the percentage of cells in each box. Cells with multiple rounds of proliferation (CFSE^{lo}) are boxed in red. Line graphs show intracellular staining for T-bet in CFSE^{lo} cells. (**B**) Analyses of T-bet change in mean fluorescence intensity (ΔMFI) are summarized in three independent experiments for a total of 12 mice for C57BL/6, 6 mice for *I-Ab*$^{-/-}$, and 12 mice for *Cd40*$^{-/-}$. (**C**) Spleen cells from 22-mo-old *Cd154*$^{-/-}$ mice were gated on live B220$^+$ cells. A representative dot plot shows the absence of ABCs (CD23$^-$CD21$^-$). Numbers represent the percentage of B cells in each population. (**D**) Absolute B cell numbers of the indicated cell subset from old C57BL/6 and *Cd154*$^{-/-}$ mice. Error bars signify the SD of values from 31 C57BL/6 mice and 5 *Cd154*$^{-/-}$ mice. The *p* values were calculated by an unpaired, equal variance Student *t* test.

did C57BL/6 cells of the same division cohort. Analyses of multiple mice (Fig. 1B) confirmed a significant increase in T-bet mean fluorescence intensity in $CFSE^{lo}$ cells compared with $CFSE^{hi}$ cells from C57BL/6 donors, whereas cells from *I-Ab*$^{-/-}$ and *Cd40*$^{-/-}$ donors had no increase. The data suggest that ABCs arise from B cells involved in immune responses to T-dependent Ags, because cognate Ag-presenting capacity and competence to receive CD40 costimulation are required. This interpretation further predicts that CD154-deficient mice, which lack CD40L, should have reduced ABC accumulation. Consistent with this expectation, analysis of splenic B cells from 22-mo-old CD154-deficient mice revealed a paucity of ABCs (Fig. 1C), despite no change in FO and MZ compartments compared with controls (Fig. 1D). Collectively, these results show that ABCs are generated slowly after endogenous Ag presentation via MHC class II and costimulation via the CD40 receptor with CD40L on T cells. The notion that ABCs are derived from T-dependent immune responses raises questions about the breadth and nature of potential Ags involved in their generation and whether they bear hallmarks of germinal center participation. Accordingly, we interrogated Ig variable (V) gene usage and levels of somatic hypermutation among quiescent, naturally occurring ABCs from old mice.

ABCs exhibit a diverse V gene segment repertoire

ABC accumulation may reflect the aggregate of immune responses to a large and diverse class of endogenous Ags and, thus, involve a broad array of clonotypic specificities. Alternatively, accumulation could be mediated by common exposure to a limited array of self- or environmental ligands that generate oligoclonal expansions with limited repertoire diversity. To differentiate between these possibilities, we sorted FO, MZ, and ABC B cell subsets from 22-mo-old mice and compared V_H and Vκ gene segment usage. Because the majority of ABCs express IgM (9), sequencing analyses for H chain genes were done on cDNA amplified with a Cμ 3′ primer and degenerate V_H 5′ primers. Likewise, κ L chain genes were identified by amplifying cDNA with a Cκ 3′ primer and degenerate Vκ 5′ primers. Some 2400 unique sequences for both loci were collected and analyzed. Overall, the usage of V_H and Vκ gene segments was similar among all three subsets. For V_H genes, 85 genes from 12 families were identified, and their frequencies were measured within the subsets. ABCs were compared separately with FO (Fig. 2A) and MZ (Fig. 2B) cells, and significant differences in over- or underutilization were seen in only two to four individual genes. For Vκ genes, 69 genes from 15 families were found; when ABCs were compared with FO (Fig. 3A) or MZ (Fig. 3B) cells, only three to five genes were significantly over- or underused. Thus, there was no evidence for strong repertoire skewing, arguing against a restricted Ag-driven response. We also did not observe significant selection for amino acid replacement changes in CDRs for Ig H chain and Igκ-chains from the ABC population (data not shown). These results suggest that ABCs develop in response to a broad range of Ags.

ABC V genes have undergone somatic hypermutation

The requirement for CD40–CD154 interactions in ABC accumulation suggests that most ABCs are products of activation involving cognate T cell help. If so, the V genes of ABCs should contain increased frequencies of mutations compared with other subsets. To

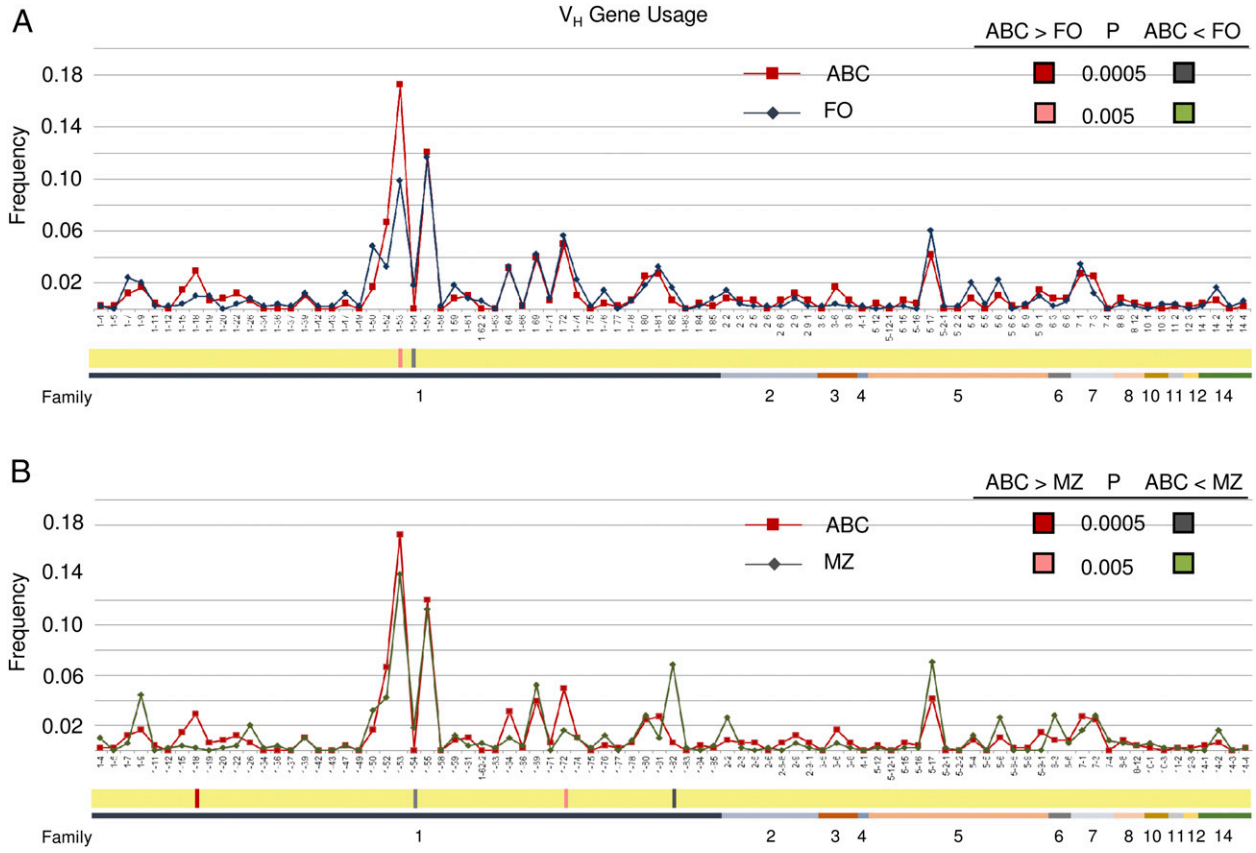

FIGURE 2. Diverse V_H gene segment usage in ABCs. The frequency of gene expression within the indicated B cell population in old mice (n = 18–24 mice for FO, MZ, and ABC subsets) was determined using RT-PCR. For each subset, ~400 V_H sequences were analyzed. V genes were grouped by family, which is indicated numerically below the graph. Significant differences in V gene usage between ABC and FO (**A**) or between ABC and MZ (**B**) subsets were calculated using the Fisher exact test and are shown below the gene name in the yellow bar. The p value heat map scale is shown.

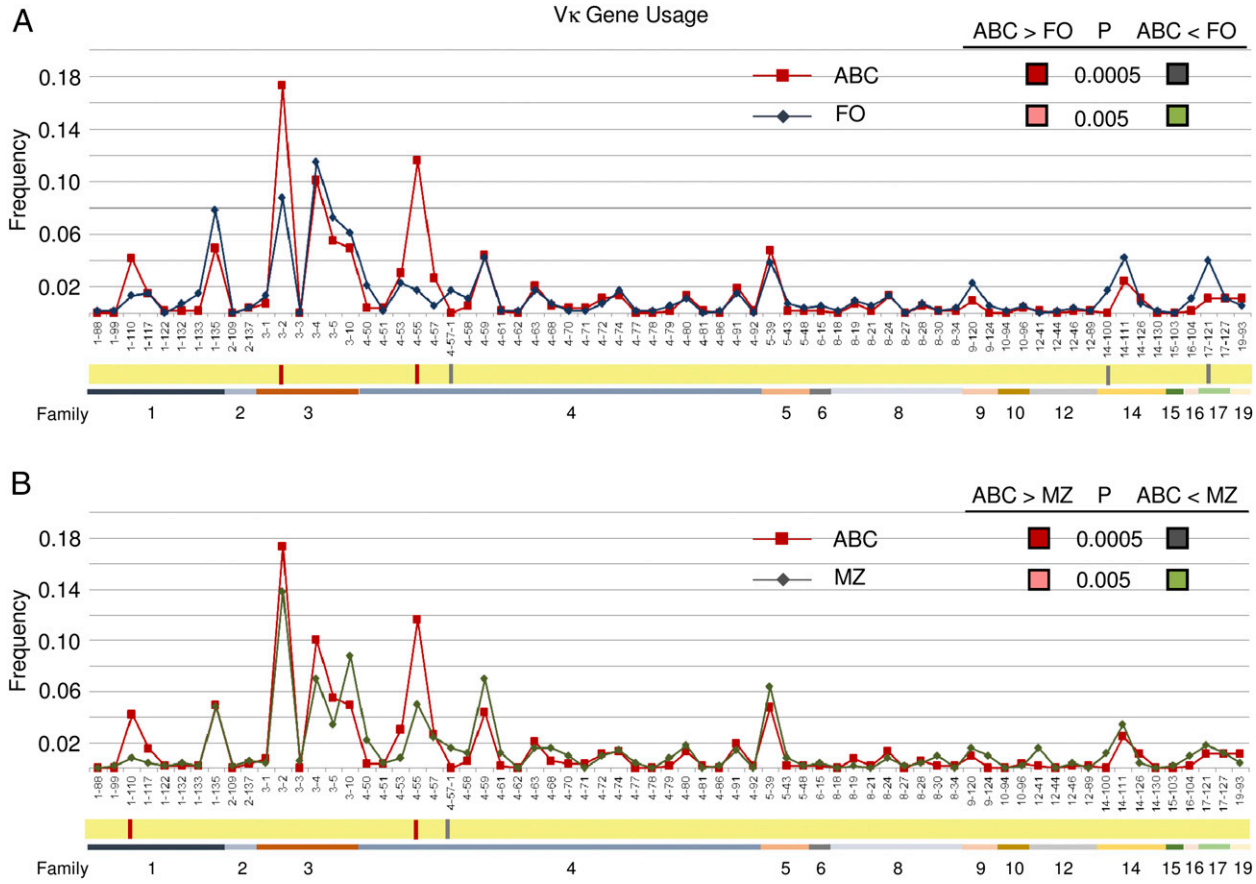

FIGURE 3. Diverse Vκ gene segment usage in ABCs. (**A**) ABC vs. FO subsets. (**B**) ABC vs. MZ subsets. Details are similar to Fig. 2 legend.

address this, we counted the number of mutations in VDJ heavy and VJ κ light exons amplified from FO, MZ, and ABC B cell subsets from 22-mo-old mice used for the repertoire analysis. Sequences of V, D, and J gene segments were compared with their germline counterparts to identify mutations. VDJ and VJ genes from ABCs had a significant 4-fold increase in mutations compared with FO cells and a significant 2-fold increase compared with MZ cells (Fig. 4A, 4B). As a control, V exons were sequenced from FO and MZ cells from young *Aid*$^{-/-}$ mice, which cannot undergo hypermutation because the activation-induced deaminase protein is absent. The mutation frequency was ~2×10^{-3} mutations per base pair for activation-induced deaminase–deficient cells, which represents the background frequency of errors produced during cDNA synthesis and PCR amplification. The distribution of mutations per sequence is shown in Fig. 4C, which shows that two thirds of sequences from ABCs had mutations, indicating that most of these B cells have encountered some type of Ag during their existence. An examination of the types of nucleotide substitutions in the cadre of >2700 mutations from VDJ and VJ genes from the ABC sequences showed no difference compared with FO and MZ substitutions (data not shown). Because the error rate for sequencing cDNA clones from RNA is elevated due to errors from the low-fidelity reverse transcriptase used to make cDNA, we also analyzed mutations in the 492-bp J_H4 intronic region directly from DNA, using a high-fidelity polymerase. FO, MZ, and ABC B cell subsets were sorted as described above, and the J_H4 region was amplified from genomic DNA. As shown in Fig. 4D–F, there was a significant increase in mutation frequency from ABCs compared with those from FO and MZ cells, confirming that ABCs have undergone somatic hypermutation. As a control, introns were sequenced from germinal center B cells of young mice taken 4 wk after immunization with (4-hydroxy-3-nitrophenyl) acetyl–chicken γ globulin (24), and the frequency was 5-fold higher than in ABCs. This comparison places ABCs in the middle between naive and germinal center cells, suggesting that they undergo mild chronic stimulation by endogenous Ags versus acute stimulation by immunization.

Some Ag-specific B cells express T-bet and CD11c

Our results suggest an Ag-driven origin for ABCs that, coupled with their continuous accumulation, BLyS independence, and resting state (9, 25), lends credence to the idea that they are an unusual subset of B cells. To further interrogate the provenance of ABCs, we compared their gene-expression profiles with those from FO B cells sorted from old and young mice. ABC uniqueness is shown by a subset of 70 genes with ≥5-fold higher expression in old ABCs compared with old and young FO B cells (Supplemental Fig. 1A, Supplemental Table I). T-bet and CD11c were overexpressed in ABCs, confirming previous reports (13, 14). Principal component analysis was used to visualize intersample variation among all of the genes from sorted subsets and illustrated that old ABCs have distinct gene-expression profiles compared with FO B cells from old and young mice (Supplemental Fig. 1B).

Based on their accumulation of somatic hypermutation, we hypothesized that ABCs represent a subset of Ag-experienced B cells whose accretion reflects the cumulative aggregate of challenges that drive their formation. To demonstrate that another subset of Ag-experienced B cells arising from deliberate infection also expresses T-bet and CD11c, we infected young mice with influenza. HA-specific B cells were tracked by binding to fluorescent labeled HA-PE. Prior to infection, the frequency of HA-reactive B cells was low (Fig. 5A), consistent with prior estimates of ~1/50,000 splenic B cells (26). Following infection, mice displayed the expected

A

Cell type	Sequences	Nucleotides	Mutations	Frequency x 10^{-3}
VDJ exon				
FO	476	139,944	430	3.1
MZ	419	121,929	703	5.8
ABC	372	108,624	1,443	13.3
VJ exon				
FO	460	132,940	419	3.2
MZ	395	112,575	872	7.7
ABC	340	98,600	1,296	13.1

D

Cell type	Sequences	Nucleotides	Mutations	Frequency x 10^{-3}
J_H4 intron				
FO	301	147,791	65	0.4
MZ	301	147,791	90	0.6
ABC	294	144,354	218	1.5

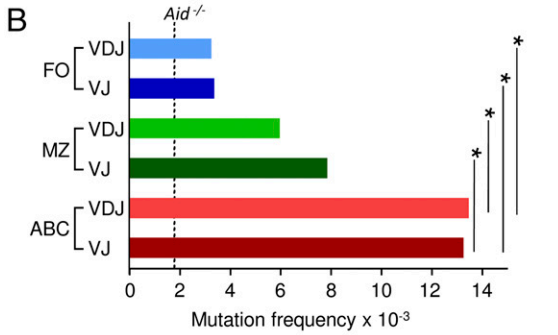

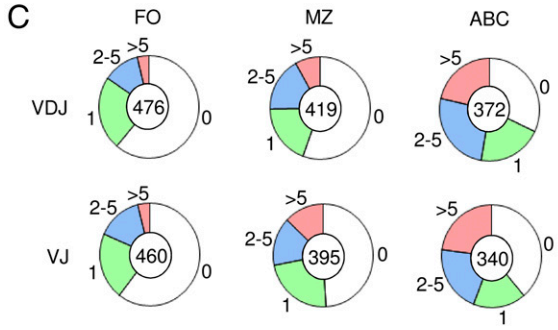

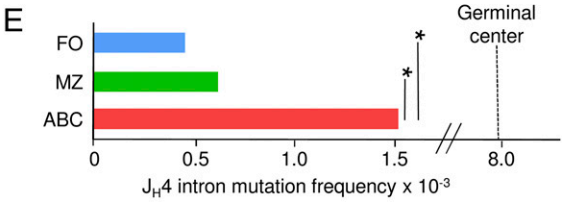

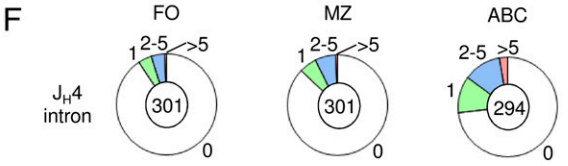

FIGURE 4. ABCs have increased somatic hypermutation. (**A**–**C**) Exon sequences from Figs. 2 and 3 were analyzed for mutations in rearranged VDJ genes for the H chain and in rearranged VJ genes for the κ L chain. (A) Numbers of unique sequences, nucleotides, mutations, and frequencies. (B) Mean mutation frequencies (mutations/nucleotides) in the exons of each B cell subset were calculated. The dotted line indicates the mutation frequency in *Aid*$^{-/-}$ FO and MZ B cells from young mice. (C) Distribution of mutations per sequence. The number of sequences is shown in the center of each circle. Segments represent the proportion of sequences that contain the indicated number of mutations. (**D**–**F**) J_H4 intron sequences were analyzed from genomic DNA of 11–13 mice for each subset. (D). Numbers of sequences, nucleotides, mutations, and frequencies. (E) Mean mutation frequencies; the dotted line represents the frequency in germinal centers from young immunized mice. (F) Distribution of mutations per sequence. *$p < 0.0001$, χ^2 test.

weight loss and fully recovered 30 d later (Fig. 5B), indicating that the virus was cleared. At day 100 postinfection, HA-reactive B cells increased, and ~25% of these were T-bet$^+$CD11c$^+$ (Fig. 5C, 5D). Collectively, these observations on influenza-infected mice support the analogy that some long-lived Ag-experienced cells express the phenotype associated with ABCs.

Discussion

These studies probe the origin and nature of ABCs, a B cell subset that steadily accumulates with age and whose surface phenotype and transcriptional signature were associated with humoral autoimmunity and antipathogen immune responses. We provide three lines of evidence that ABCs are a unique B cell subset. First, adoptive-transfer studies using MHC class II and CD40-deficient cells confirm our prior report that young FO B cells can give rise to ABCs after extensive division (9) and extend this observation in several ways. Notably, they demonstrate that ABCs can be generated with cognate T cell help, which is substantiated by the lack of ABCs in old *CD154*$^{-/-}$ mice. These findings also significantly connect T-bet expression with these extensively divided cells, a feature that is well established in ABC genesis (12, 13). In addition, our results indicate that homeostatic expansion is unlikely to be the major source of ABCs. The transfer experiments involved replete hosts, with minimal space for donor cells to fill by division, and the relatively few transferred cells from MHC class II– and CD40-deficient donors that divided did not express T-bet. Overall, our data support the hypothesis that most ABCs are the cumulative result of enduring environmental Ag stimulation through T-dependent mechanisms. However, the results do not exclude a TLR-mediated origin for some ABCs that may respond to viral or autoimmune stimuli (27).

Second, analyses of V gene segment use and somatic hypermutation indicate encounters with multiple Ags. The breadth of V-gene usage speaks against a monolithic origin in terms of Ag or epitope recognition and demonstrates that ABCs represent a cross-section of responses to a broad array of Ags. Numerous early reports suggested that the total B cell repertoire was restricted in old mice (5, 28–31). However, our extensive analysis of 85 V_H gene segments and 69 Vκ gene segments revealed a rich spectrum of V-gene usage by FO, MZ, and ABCs from old mice, indicating that global sequencing generates a more comprehensive view of the repertoire than do limited studies of Ag-specific cells. Only a handful of genes were over- or underused by ABCs; overall, there was no significant difference when ABCs were compared with FO

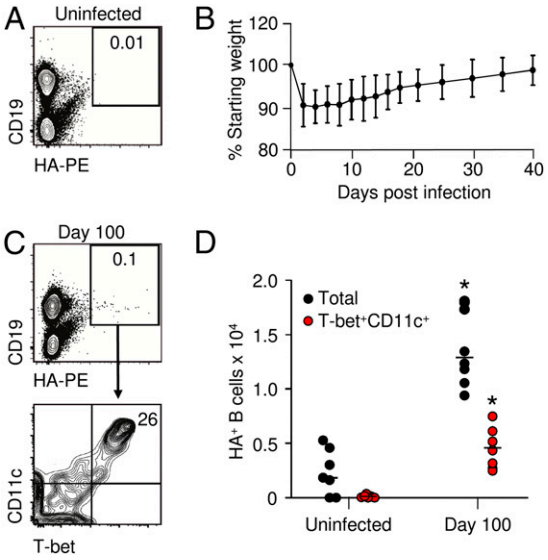

FIGURE 5. B cells infected with influenza HA express T-bet and CD11c. Mice were infected intranasally with PR8, and spleens were harvested 100 d postinfection. (**A**) Representative profile of HA-PE–binding B cells ($CD19^+$) in an uninfected spleen. Number shows the percentage of cells in highlighted box. (**B**) Weight loss and recovery postinfection. Error bars signify SD from eight mice. (**C**) Gating profile for HA-binding B cells in spleens at day 100 (upper panel). Number in box reflects the percentage of cells. A portion of HA-binding B cells express T-bet and CD11c (lower panel). (**D**) Number of B cells that bind HA. Total $T\text{-}bet^-CD11c^-$ and $T\text{-}bet^+CD11c^+$ cells (black circles) compared with only $T\text{-}bet^+CD11c^+$ cells (red circles). Data are from seven uninfected and eight d-100 infected mice collected in three independent experiments. $*p < 0.01$, uninfected versus infected groups, unpaired equal-variance Student *t* test.

or MZ repertoires. Such results would be expected if multiple heterogeneous Ags generated the diverse repertoire. Possible candidates are self-antigens or Ags of the microbiota environment. With regard to self-antigens, a previous report found that mice stimulated chronically with TLR7 agonists developed ABCs expressing high titers of anti-Smith autoimmune Abs (10). However, the few genes that were overused in ABCs in this study did not possess positively charged CDR3 regions in their rearranged sequences, which are common in self-reactive Abs (32). It appears that healthy old mice without deliberate immunization develop a heterogeneous repertoire, without propensity for autoimmune Abs. Although the repertoires of ABCs, FO cells, and MZ cells were similar, the results of the mutation analyses were strikingly different. ABCs showed clear evidence of mutation in the V_H and Vκ exons compared with FO and MZ B cells. Although FO B cells had the lowest mutation frequency, consistent with their pre-immune status, the frequency was 2-fold higher in MZ cells, which have likely encountered microbial Ags during circulation, and 4-fold higher in ABCs. In ABCs, mutations did not accumulate in CDRs, consistent with the lack of selection of certain V genes in the repertoire analysis. Furthermore, there was a significant increase in mutation frequency in ABCs in the noncoding J_H4 intron, which is a broad substrate for hypermutation in the absence of selection (33). However, it remains uncertain whether all ABCs are the products of germinal center reactions. For example, most ABCs have IgM receptors and continue to express the surface receptor TACI (9), both of which are inconsistent with the germinal center B cell phenotypes (34). Moreover, the mutation frequency in ABCs was lower compared with germinal center B cells from immunized mice (24). There is precedent for mutated IgM-bearing cells occurring in the absence of germinal centers (35, 36). Alternatively, ABCs may represent early germinal center emigrants that exit before concerted selection (37, 38).

Third, microarray analyses of gene expression show that ABCs from old mice are unique in relation to FO cells from young and old mice. Transcription analysis was also performed by Rubtsov et al. (10) to compare old ABCs with old FO, old B1, and young B1 cells. However, the two analyses profile different sets of genes because the cells were isolated under different conditions. The ABCs in the study from Rubtsov et al. (10) were sorted for $CD11b^+$ expression, and the ABCs analyzed in this study were sorted as $CD21^-$ $CD23^-$. Nonetheless, both analyses show that T-bet and CD11c are greatly increased in old ABCs relative to old FO cells. We found that this signature was also present in some long-lived B cells following influenza infection 100 d later, confirming our previous report (39). By analogy, ABCs are Ag experienced, because they have increased somatic hypermutation, and they require T cell interactions for their generation. The cells presumably arise from chronic stimulation by endogenous Ags, but it is important to note that ABCs are resting cells that persist over time. Whether they can undergo recall responses when they encounter cognate Ags remains to be determined.

Acknowledgments

We thank Robert Maul, Ranjan Sen, and Diana Castiblanco for stimulating conversations and advice, William Yang for technical assistance, and Kate Turlington, Haleigh Larson, and Arielle Kilner for experiments. Robert Wersto, Jade Scheers, Tonya Wallace, and Cuong Nguyen (National Institute on Aging Flow Cytometry Core Facility) assisted in cell sorting. Michael Paley and E. John Wherry (University of Pennsylvania) assisted with the ABC/FO microarray and initial analyses.

Disclosures

The authors have no financial conflicts of interest.

References

1. Miller, J. P., and D. Allman. 2003. The decline in B lymphopoiesis in aged mice reflects loss of very early B-lineage precursors. *J. Immunol.* 171: 2326–2330.
2. Cancro, M. P. 2005. B cells and aging: gauging the interplay of generative, selective, and homeostatic events. *Immunol. Rev.* 205: 48–59.
3. Miller, J. P., and M. P. Cancro. 2007. B cells and aging: balancing the homeostatic equation. *Exp. Gerontol.* 42: 396–399.
4. Kline, G. H., T. A. Hayden, and N. R. Klinman. 1999. B cell maintenance in aged mice reflects both increased B cell longevity and decreased B cell generation. *J. Immunol.* 162: 3342–3349.
5. Johnson, S. A., S. J. Rozzo, and J. C. Cambier. 2002. Aging-dependent exclusion of antigen-inexperienced cells from the peripheral B cell repertoire. *J. Immunol.* 168: 5014–5023.
6. Zheng, B., S. Han, Y. Takahashi, and G. Kelsoe. 1997. Immunosenescence and germinal center reaction. *Immunol. Rev.* 160: 63–77.
7. Frasca, D., and B. B. Blomberg. 2011. Aging impairs murine B cell differentiation and function in primary and secondary lymphoid tissues. *Aging Dis.* 2: 361–373.
8. Goenka, R., J. L. Scholz, M. S. Naradikian, and M. P. Cancro. 2014. Memory B cells form in aged mice despite impaired affinity maturation and germinal center kinetics. *Exp. Gerontol.* 54: 109–115.
9. Hao, Y., P. O'Neill, M. S. Naradikian, J. L. Scholz, and M. P. Cancro. 2011. A B-cell subset uniquely responsive to innate stimuli accumulates in aged mice. *Blood* 118: 1294–1304.
10. Rubtsov, A. V., K. Rubtsova, A. Fischer, R. T. Meehan, J. Z. Gillis, J. W. Kappler, and P. Marrack. 2011. Toll-like receptor 7 (TLR7)-driven accumulation of a novel $CD11c^+$ B-cell population is important for the development of autoimmunity. *Blood* 118: 1305–1315.
11. Ratliff, M., S. Alter, D. Frasca, B. B. Blomberg, and R. L. Riley. 2013. In senescence, age-associated B cells secrete TNFα and inhibit survival of B-cell precursors. *Aging Cell* 12: 303–311.
12. Rubtsova, K., A. V. Rubtsov, M. P. Cancro, and P. Marrack. 2015. Age-associated B cells: a T-bet-dependent effector with roles in protective and pathogenic immunity. *J. Immunol.* 195: 1933–1937.
13. Rubtsova, K., A. V. Rubtsov, L. F. van Dyk, J. W. Kappler, and P. Marrack. 2013. T-box transcription factor T-bet, a key player in a unique type of B-cell activation essential for effective viral clearance. *Proc. Natl. Acad. Sci. USA* 110: E3216–E3224.
14. Rubtsov, A. V., K. Rubtsova, J. W. Kappler, J. Jacobelli, R. S. Friedman, and P. Marrack. 2015. CD11c-expressing B cells are located at the T cell/B cell border in spleen and are potent APCs. *J. Immunol.* 195: 71–79.

15. Ratliff, M., S. Alter, K. McAvoy, D. Frasca, J. A. Wright, S. S. Zinkel, W. N. Khan, B. B. Blomberg, and R. L. Riley. 2015. In aged mice, low surrogate light chain promotes pro-B-cell apoptotic resistance, compromises the PreBCR checkpoint, and favors generation of autoreactive, phosphorylcholine-specific B cells. *Aging Cell* 14: 382–390.
16. Claes, N., J. Fraussen, M. Vanheusden, N. Hellings, P. Stinissen, B. Van Wijmeersch, R. Hupperts, and V. Somers. 2016. Age-associated B cells with proinflammatory characteristics are expanded in a proportion of multiple sclerosis patients. *J. Immunol.* 197: 4576–4583.
17. Moir, S., J. Ho, A. Malaspina, W. Wang, A. C. DiPoto, M. A. O'Shea, G. Roby, S. Kottilil, J. Arthos, M. A. Proschan, et al. 2008. Evidence for HIV-associated B cell exhaustion in a dysfunctional memory B cell compartment in HIV-infected viremic individuals. *J. Exp. Med.* 205: 1797–1805.
18. Weiss, G. E., P. D. Crompton, S. Li, L. A. Walsh, S. Moir, B. Traore, K. Kayentao, A. Ongoiba, O. K. Doumbo, and S. K. Pierce. 2009. Atypical memory B cells are greatly expanded in individuals living in a malaria-endemic area. *J. Immunol.* 183: 2176–2182.
19. Zinöcker, S., C. E. Schindler, J. Skinner, T. Rogosch, M. Waisberg, J. N. Schickel, E. Meffre, K. Kayentao, A. Ongoïba, B. Traoré, and S. K. Pierce. 2015. The V gene repertoires of classical and atypical memory B cells in malaria-susceptible West African children. *J. Immunol.* 194: 929–939.
20. Portugal, S., C. M. Tipton, H. Sohn, Y. Kone, J. Wang, S. Li, J. Skinner, K. Virtaneva, D. E. Sturdevant, S. F. Porcella, et al. 2015. Malaria-associated atypical memory B cells exhibit markedly reduced B cell receptor signaling and effector function. *ELife* 8: 4.
21. Yates, J. L., R. Racine, K. M. McBride, and G. M. Winslow. 2013. T cell-dependent IgM memory B cells generated during bacterial infection are required for IgG responses to antigen challenge. *J. Immunol.* 191: 1240–1249.
22. Wang, Z., M. Raifu, M. Howard, L. Smith, D. Hansen, R. Goldsby, and D. Ratner. 2000. Universal PCR amplification of mouse immunoglobulin gene variable regions: the design of degenerate primers and an assessment of the effect of DNA polymerase 3′ to 5′ exonuclease activity. *J. Immunol. Methods* 233: 167–177.
23. Whittle, J. R., A. K. Wheatley, L. Wu, D. Lingwood, M. Kanekiyo, S. S. Ma, S. R. Narpala, H. M. Yassine, G. M. Frank, J. W. Yewdell, et al. 2014. Flow cytometry reveals that H5N1 vaccination elicits cross-reactive stem-directed antibodies from multiple Ig heavy-chain lineages. *J. Virol.* 88: 4047–4057.
24. Zanotti, K. J., R. W. Maul, D. P. Castiblanco, W. Yang, Y. J. Choi, J. T. Fox, K. Myung, H. Saribasak, and P. J. Gearhart. 2015. ATAD5 deficiency decreases B cell division and Igh recombination. *J. Immunol.* 194: 35–42.
25. Scholz, J. L., J. E. Crowley, M. M. Tomayko, N. Steinel, P. J. O'Neill, W. J. Quinn, III, R. Goenka, J. P. Miller, Y. H. Cho, V. Long, et al. 2008. BLyS inhibition eliminates primary B cells but leaves natural and acquired humoral immunity intact. *Proc. Natl. Acad. Sci. USA* 105: 15517–15522.
26. Cancro, M. P., W. Gerhard, and N. R. Klinman. 1978. The diversity of the influenza-specific primary B-cell repertoire in BALB/c mice. *J. Exp. Med.* 147: 776–787.
27. Naradikian, M. S., Y. Hao, and M. P. Cancro. 2016. Age-associated B cells: key mediators of both protective and autoreactive humoral responses. *Immunol. Rev.* 269: 118–129.
28. Viale, A. C., J. A. Chies, F. Huetz, E. Malenchere, M. Weksler, A. A. Freitas, and A. Coutinho. 1994. VH-gene family dominance in ageing mice. *Scand. J. Immunol.* 39: 184–188.
29. Ben-Yehuda, A., P. Szabo, J. LeMaoult, J. S. Manavalan, and M. E. Weksler. 1998. Increased VH 11 and VH Q52 gene use by splenic B cells in old mice associated with oligoclonal expansions of CD5+ B cells. *Mech. Ageing Dev.* 103: 111–121.
30. Riley, S. C., B. G. Froscher, P. J. Linton, D. Zharhary, K. Marcu, and N. R. Klinman. 1989. Altered VH gene segment utilization in the response to phosphorylcholine by aged mice. *J. Immunol.* 143: 3798–3805.
31. LeMaoult, J., S. Delassus, R. Dyall, J. Nikolić-Zugić, P. Kourilsky, and M. E. Weksler. 1997. Clonal expansions of B lymphocytes in old mice. *J. Immunol.* 159: 3866–3874.
32. Wardemann, H., S. Yurasov, A. Schaefer, J. W. Young, E. Meffre, and M. C. Nussenzweig. 2003. Predominant autoantibody production by early human B cell precursors. *Science* 301: 1374–1377.
33. Lebecque, S. G., and P. J. Gearhart. 1990. Boundaries of somatic mutation in rearranged immunoglobulin genes: 5′ boundary is near the promoter, and 3′ boundary is approximately 1 kb from V(D)J gene. *J. Exp. Med.* 172: 1717–1727.
34. Goenka, R., A. H. Matthews, B. Zhang, P. J. O'Neill, J. L. Scholz, T. S. Migone, W. J. Leonard, W. Stohl, U. Hershberg, and M. P. Cancro. 2014. Local BLyS production by T follicular cells mediates retention of high affinity B cells during affinity maturation. *J. Exp. Med.* 211: 45–56.
35. Voigt, I., S. A. Camacho, B. A. de Boer, M. Lipp, R. Förster, and C. Berek. 2000. CXCR5-deficient mice develop functional germinal centers in the splenic T cell zone. *Eur. J. Immunol.* 30: 560–567.
36. Di Niro, R., S. J. Lee, J. A. Vander Heiden, R. A. Elsner, N. Trivedi, J. M. Bannock, N. T. Gupta, S. H. Kleinstein, F. Vigneault, T. J. Gilbert, et al. 2015. *Salmonella* infection drives promiscuous B cell activation followed by extrafollicular affinity maturation. *Immunity* 43: 120–131.
37. Pape, K. A., J. J. Taylor, R. W. Maul, P. J. Gearhart, and M. K. Jenkins. 2011. Different B cell populations mediate early and late memory during an endogenous immune response. *Science* 331: 1203–1207.
38. Weisel, F. J., G. V. Zuccarino-Catania, M. Chikina, and M. J. Shlomchik. 2016. A temporal switch in the germinal center determines differential output of memory B and plasma cells. *Immunity* 44: 116–130.
39. Naradikian, M. S., A. Myles, D. P. Beiting, K. J. Roberts, L. Dawson, R. S. Herati, B. Bengsch, S. L. Linderman, E. Stelekati, R. Spolski, et al. 2016. Cutting edge: IL-4, IL-21, and IFN-γ interact to govern T-bet and CD11c expression in TLR-activated B cells. *J. Immunol.* 197: 1023–1028.

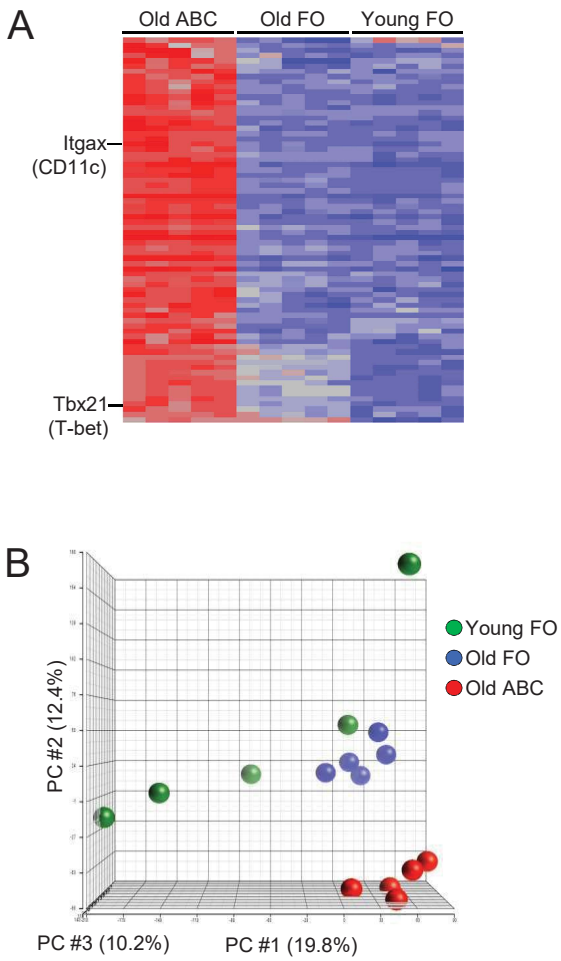

FIGURE S1. ABCs display a distinct gene expression profile.
(A) Heat map showing relative expression levels of transcripts that are at least 5-fold higher (red) in old ABCs compared to old FO B cells or young FO cells (blue). Gene names are provided in Table S1. (**B**) Principal component analysis of all genes expressed in young FO, old FO, and old ABC, sorted from 5 young and 5 old mice. The first, second, and third components account for 42.4% of the variance in the data matrix.

Table S1. List of transcripts ≥ 5-fold higher in old ABC compared to old FO (shown in Fig. S1A)

Gene symbol	Gene name
Rgs1	regulator of G-protein signaling 1
Ccl19	chemokine (C-C motif) ligand 19
Ctla4	cytotoxic T-lymphocyte-associated protein 4
Il10	interleukin 10
Fam46c	family with sequence similarity 46, member C
Id2	inhibitor of DNA binding 2
S1pr3	sphingosine-1-phosphate receptor 3
Sh2d1b1	SH2 domain containing 1B1
Abcb1b	ATP-binding cassette, sub-family B (MDR/TAP), member 1B
Ramp3	receptor (calcitonin) activity modifying protein 3
Nrp2	neuropilin 2
Parm1	prostate androgen-regulated mucin-like protein 1
Havcr1	hepatitis A virus cellular receptor 1
Anxa2	Mouse annexin
Rbm47	RNA binding motif protein 47
Chn2	chimerin 2
Nt5e	5' nucleotidase, ecto
Il2rb	interleukin 2 receptor, beta chain
Art3	ADP-ribosyltransferase 3
4930506M07Rik	shootin 1
Itgax	integrin alpha X (CD11c)
Cxcl10	chemokine (C-X-C motif) ligand 10
Ptpn22	protein tyrosine phosphatase, non-receptor type 22 (lymphoid)
Cd300lf	CD300 molecule like family member F
Gm5486	M. musculus predicted gene 5486
Sirpa	signal-regulatory protein alpha
Zbtb32	zinc finger and BTB domain containing 32
Cd80	CD80 antigen
Gm1965	M. musculus predicted gene 1965
Cd80	CD80 antigen (RIKEN library)
Gpr55	G protein-coupled receptor 55
Cdk14	cyclin-dependent kinase 14
Lcp2	lymphocyte cytosolic protein 2
Emr1	adhesion G protein-coupled receptor E1 (Adgre1)
Itgb1	integrin beta 1 (fibronectin receptor beta)
Zeb2	zinc finger E-box binding homeobox 2
Bmpr1a	bone morphogenetic protein receptor, type 1A
Fgl2	fibrinogen-like protein 2
Lilrb4	leukocyte immunoglobulin-like receptor, subfamily B, member 4A
Zbtb20	zinc finger and BTB domain containing 20
Rcn3	reticulocalbin 3, EF-hand calcium binding domain
Fah	fumarylacetoacetate hydrolase
Zbtb20	zinc finger and BTB domain containing 20
Fcer1g	Fc receptor, IgE, high affinity I, gamma polypeptide
Itm2c	integral membrane protein 2C
Ptpn14	protein tyrosine phosphatase, non-receptor type 14
Grk5	G protein-coupled receptor kinase 5
Zc3h12c	zinc finger CCCH type containing 12C
Gp49a	leukocyte immunoglobulin-like receptor, subfamily B, member 4B
Bhlhe41	basic helix-loop-helix family, member e41
Apoe	apolipoprotein E
Itgam	integrin alpha M
Ahnak	AHNAK nucleoprotein (desmoyokin)
Cd3g	CD3 antigen, gamma polypeptide
Lgals1	lectin, galactose binding, soluble 1
AK081116	Hypothetical Gag gene protein p24
Apoc2	apolipoprotein C-II
Plscr1	phospholipid scramblase 1
LOC100041877	nuclear body protein SP140-like
Naip5	NLR family, apoptosis inhibitory protein 5
Fcrl5	Fc receptor-like 5
Trabd2b	TraB domain containing 2B
Naip6	NLR family, apoptosis inhibitory protein 6
Atxn1	ataxin 1
Gm7609	predicted pseudogene 7609 (Gm7609)
Ackr2	atypical chemokine receptor 2
Tbx21	T-box 21 (T-bet)
Fas	Fas (TNF receptor superfamily member 6)
Mpeg1	macrophage expressed gene 1
G530011O06Rik	RIKEN cDNA G530011O06 gene

Gene names are from the NCBI Nucleotide or Ensembl databases. Transcripts are listed in order from top to bottom of Fig. S1A. Duplicates either map to different clones of the same gene (CD80, Zbtb20) or are repeats of the same RefSeq (Gm1965, Gm7609, Plscr1, Zc3h12c). This dataset is available through the NCBI GEO repository (dataset GSE81650).